



HAL
open science

Concomitant effects of light and temperature diel variations on the growth rate and lipid production of *Dunaliella salina*

Hubert Bonnefond, N. Moelants, Amélie Talec, Olivier Bernard, A. Sciandra

► **To cite this version:**

Hubert Bonnefond, N. Moelants, Amélie Talec, Olivier Bernard, A. Sciandra. Concomitant effects of light and temperature diel variations on the growth rate and lipid production of *Dunaliella salina*. *Algal Research - Biomass, Biofuels and Bioproducts*, 2016, 14, pp.72-78. 10.1016/j.algal.2015.12.018 . hal-01266717

HAL Id: hal-01266717

<https://hal.sorbonne-universite.fr/hal-01266717>

Submitted on 3 Feb 2016

HAL is a multi-disciplinary open access archive for the deposit and dissemination of scientific research documents, whether they are published or not. The documents may come from teaching and research institutions in France or abroad, or from public or private research centers.

L'archive ouverte pluridisciplinaire **HAL**, est destinée au dépôt et à la diffusion de documents scientifiques de niveau recherche, publiés ou non, émanant des établissements d'enseignement et de recherche français ou étrangers, des laboratoires publics ou privés.

1 **Concomitant effects of light and temperature diel variations on the growth**
2 **rate and lipid production of *Dunaliella salina***

3 Bonnefond H^a, Moelants N^a, Talec A^a, Bernard O^b, Sciandra A^{a,b}

4 ^a Sorbonne Universités, UPMC Univ Paris 06, INSU-CNRS, Laboratoire d'Océanographie de Villefranche,
5 181 Chemin du Lazaret, 06230 Villefranche-sur-mer, France

6 ^b INRIA BIOCORE, 06902 Sophia Antipolis, France

7 **Abstract**

8 The microalgae *Dunaliella salina* has the capacity to grow in salterns at high salinity. In this
9 particular shallow environment, *D. salina* is exposed to strong light and temperature
10 variations and has developed various strategies such as cell cycle adaptation and storage of
11 dedicated metabolites. The effects of light/dark cycles have already been studied, but few
12 works focused on the concomitant effects of light and temperature variations characterizing
13 salterns and outdoor conditions. In this study, growth, carbon and nitrogen storage,
14 pigments and lipid production of *D. Salina* was measured, in laboratory conditions mimicking
15 the outdoor light and temperature conditions. A control experiment with constant
16 temperature was carried out with light variations only. During the night, cell respiration was
17 correlated with temperature, following an Arrhenius law. Many differences with the control
18 at constant temperature confirmed that temperature variations are a crucial parameter in
19 outdoor conditions and should be taken into account to predict growth. Triglycerides and
20 pigments production was tightly linked to the light dark cycle.

21 **1. Introduction**

22 Microalgae have developed numerous mechanisms to permanently adapt to a fluctuating
23 environment. Key points for survival in periodic conditions are cell cycle synchronization with

24 light and temperature [1]. The first consequence of this adaptation is the modulation of
25 carbon and nitrogen acquisition during the cell cycle [2]. The second comprises daily
26 dynamics of storage metabolites like lipids, [3, 4]. The green microalgae *D. salina* grows in
27 salt lakes or in shallow salterns and tolerates wide ranges of salinity, between 0.5 M to 5 M
28 [5]. Due to low water depth, this species has adapted its metabolism and cell cycle to high
29 temperature and light variations over a course of a day. To survive within a changing
30 environment, *Dunaliella sp* produces different compounds. Carotenoids, such as beta-
31 carotene and lutein, are accessory pigments used as photoprotectors. *D. salina* is among the
32 organisms containing the highest concentrations of carotenoids after metabolic stress [6].
33 This species can also produce triglycerides (TAG) to store energy and carbon to sustain
34 growth during the night. In addition, *Dunaliella sp* synthesizes glycerol as an osmo-regulator
35 when grown in hypersaline environments [5]. Industrially, this is the third most important
36 microalgae produced in terms of dry weight (1200 t/year) after *Arthrospira sp.* and *Chlorella*
37 *sp* [7]. It is grown mainly for its carotenoids which have strong antioxidant properties that
38 are utilized in the cosmetic and nutritional markets. Its ability to accumulate triglycerides as
39 a potential source of biofuel is also gaining interest.

40 Photosynthesis is impacted by temperature and light fluctuations. The effect on inorganic
41 carbon acquisition is direct for light, and indirect for temperature, which modulate
42 enzymatic activity. The simultaneous impact of these factors needs to be studied to better
43 understand the daily pattern of carbon acquisition and storage, but also, over a longer time
44 scale, to comprehend its evolution with seasonal variations [8]. Some studies have been
45 carried out with *D. salina* to investigate the individual effects of light or temperature on
46 growth and metabolites [8, 9, 5], but the effects resulting from their concomitant variations
47 have not yet been studied. Thus the aim of this study was to investigate the effects of

48 concomitant realistic evolution of temperature and light on the metabolic response of *D.*
49 *salina*, mainly in terms of carbon and nitrogen acquisition and pigment and triglyceride
50 content. These experimental results were compared to a control experiment where
51 temperature was kept constant.

52 One of our key observations is that a periodic temperature evolution, which is rarely
53 experimentally tested, seems to strongly impact cell dynamics. The cyclic effect of
54 temperature also had a positive impact on carbon fixation.

55

56 **2. Materials and methods**

57 **2.1. Culturing system**

58 *D. salina* (CCAP 18/19) was grown in duplicate 5L, temperature-controlled water-jacketed
59 vessels previously washed with 10%HCl and rinsed with milli-Q water and sterile medium.
60 The enrichment medium was prepared in 20 L tanks (Nalgen) filled with 3 weeks matured
61 natural seawater filtered on 0.1 μm , and autoclaved at 110°C for 20 min. After cooling, f/2
62 medium was added [11]. Nitrates were added separately to the end concentration of 400
63 μM . Fresh medium filtered through a 0.22 μm sterile filter (SpiralCap, Gelman) was
64 introduced into the continuous cultures with peristaltic pumps (Gilson) at a dilution rate
65 equal to daily growth rate (Tab. 1). After inoculation, the starting cell concentration was
66 about 2×10^4 cell.mL⁻¹ and cultures were first grown in batch mode to allow the algal
67 population to increase rapidly. Then, the turbidostat mode was initiated to stabilize the
68 population at 3×10^5 cell.mL⁻¹, a concentration sufficiently high to allow accurate biochemical
69 analyses on small volume samples, and sufficiently low to prevent nutrient limitation and
70 light shading. Each day, the dilution rate (D) was checked by weighting with a precision
71 balance the input flow during 2 min and adjusted, when necessary, to maintain a constant
72 daily cell concentration. The pH was measured every minute and prevented from exceeding
73 pH 8.3 by computer-controlled micro-addition of CO₂ in the bubbling air (see [12]).
74 Homogenous cultures were maintained by gentle magnetic stirring.

75 **2.2. Light and temperature**

76 Light was provided by two arrays of six 50 cm fluorescent tubes (Dulux®1, 2G11, 55W/12-
77 950, lumilux de lux, daylight, OsramSylvania) placed on each side of the vessels.
78 Photosynthetically active radiation (PAR) was measured by a 4 π spherical collector (QSL-100,

79 Biospherical Instruments) placed between or in the two turbidostats to assure that no light
80 limitation occurred. Temperature was controlled and monitored using a temperature control
81 unit (Lauda RE 415G). Light and temperature were recorded every minute.

82 **2.3. Culture conditions**

83 A typical meteorological pattern from a meteorological station located in the Laboratory of
84 environmental biotechnology (INRA-LBE Avenue des Etangs F-11100 Narbonne, south of
85 France), was used as a concrete example of daily natural variability impacting the culture in
86 June. The daily change of temperature in the ponds was calculated by the model of [8],
87 based on this meteorological data. The L/D (14L:10D) cycle was approached by a truncated
88 sinus square function. These conditions were applied in the duplicate cultures C1-LT and C2-
89 LT (LT, for light and temperature variations), while constant temperature (at the value of
90 27°C) was applied in the duplicate cultures C3-L and C4-L (L, for light variation only ; Tab. 1).
91 The light intensity was determined to reproduce the averaged irradiance in the pond. Using
92 the Beer-Lambert law for light attenuation, the average light intensity was calculated from
93 the light at the surface, as detailed in [13].

$$I_{av} = \frac{I_{inc}}{\ln\left(\frac{I_{inc}}{I_{out}}\right)} \left(1 - \frac{I_{out}}{I_{inc}}\right) \quad (1)$$

94
95 where I_{inc} is the incident light intensity ($\mu\text{mol quanta.m}^{-2}.\text{s}^{-1}$) impinging the pond, and I_{out} the
96 light at the bottom of the raceway. We assumed here that I_{inc} at noon was such that the
97 photosynthesis rate at the bottom of the pond equaled the respiration rate, corresponding
98 to the (optimal) compensation condition defined by [14]. The compensation condition for D .

99 *salina* was determined for $I_{out} = 23 \mu\text{mol quanta}\cdot\text{m}^{-2}\cdot\text{s}^{-1}$ [6]. From (1), it followed that, for the
100 maximal incident light intensity in Narbonne, I_{inc} was $1364 \mu\text{mol quanta}\cdot\text{m}^{-2}\cdot\text{s}^{-1}$ and the
101 averaged light intensity I_{av} at noon was equal to $I_{inc}\cdot 0.22 = 300 \mu\text{mol quanta}\cdot\text{m}^{-2}\cdot\text{s}^{-1}$. These
102 conditions were obtained by a computer-controlled cultivation device able to maintain long
103 term continuous cultures [12].

104 **2.4. Cell population**

105 Cell concentration and size distribution were monitored every two hours by an automated
106 optical particle counter (HIAC - Royco; Pacific Scientific Instruments). The variability between
107 triplicate measurements was routinely lower than 5 %. The mean cell diameter of the
108 population was calculated from its size distribution. Due to high frequency acquisition,
109 continuous functions could be fitted to cell density data using Stavitzky Golay filter [15]. The
110 division rate μ (d^{-1}) was then derived according to the following equation.

$$\mu = \frac{\text{Ln}\left(\frac{n_2}{n_1}\right)}{t_2 - t_1} + D$$

111 where n_1 and n_2 are the cell concentrations ($\text{cell}\cdot\text{ml}^{-1}$) at time t_1 and t_2 , respectively, and D
112 the dilution rate (d^{-1}).

113 **2.5. Nutrient analysis**

114 Sampling for biochemical analyses were started after a culture-preconditioning period of 15
115 days, necessary for biomass stabilization and physiological adaptation of cultures to the
116 experimental conditions, and were performed consecutively during 48 hours. Nitrates (NO_3^-)
117 and nitrites (NO_2^-) concentrations were automatically measured on-line [16] to ensure that
118 the duplicate cultures were never N-limited. For particulate carbon and nitrogen analyses,
119 13.15 ml of culture were filtered in triplicates every 2 hours onto glass-fiber filters

120 (Whatman GF/C) and precombusted at 450°C for 12h. Samples were kept at 60°C until
121 analyses were performed with a CHN analyzer (2400 Series II CHNS/O, Perkin Elmer). The
122 variability between triplicate measurements was routinely lower than 6 %. Continuous
123 functions of Stavitzky Golay filter were fitted to discrete data of nitrogen and carbon
124 concentrations ($\mu\text{g}\cdot\text{mL}^{-1}$). This allows the computation of the net carbon specific fixation
125 rates of N and C, respectively ρ_N and ρ_C ($\mu\text{g}\cdot\mu\text{gC}^{-1}\cdot\text{d}^{-1}$) according to the following equation:

$$\rho_N = \frac{1}{[C]_{t_2}} \left(\frac{[N]_{t_2} - [N]_{t_1}}{(t_2 - t_1)} + D \cdot [N]_{t_2} \right)$$

126 where [N] is the particulate nitrogen concentration ($\mu\text{g}\cdot\text{mL}^{-1}$) at time t_1 and t_2 , respectively.
127 The computation of ρ_C was done similarly using particulate carbon [C] ($\mu\text{g}\cdot\text{mL}^{-1}$).

128 **2.6. Cellular content analysis**

129 Lipid analysis protocol was derived from the Bligh and Dyer's method [17]. 200 ml of culture
130 was centrifuged (JOUAN G 412) for 10 min at 2000 rpm, and the pellet was stored at -80°C
131 before lipid extraction. Two successive extractions were performed in a monophasic mixture
132 of chloroform:methanol:salt water (1:2:0.8 v/v). Chloroform and water were then added for
133 phase separation (2:2:1.8 v/v). Chloroform phase was evaporated and total lipids (TL) were
134 stored at -80°C under nitrogen atmosphere to avoid oxidation. Lipid class determination was
135 performed in triplicate after a separation step. A known mass of lipid was spotted (SES
136 A4100 Autospotter) into silica coat rods (Chromarod-SIII), then bathed with 2 successive
137 solvent mixes of hexane: benzene: formic acid (80:20:1) for 24 min and hexane: diethyl-
138 ether: formic acid (97:3:1.5) for 23 min. Following, a drying step (5 min at 110°C), lipid class
139 determination was performed with a Iatroscan (Iatroscan New MK 5 from Iatron, software :
140 Chromstar from SES Analysesystem) [18]. The variability between triplicate measurements of

141 triglycerides was routinely lower than 20 % (due to very small amount of triglyceride) and
142 less than 3% for polar lipid.

143 In the C1-LT culture, cell chlorophylls and carotenoids were sampled every 4 hours. Once
144 extracted in 100% methanol (containing Vitamin E acetate as internal standard) for 2 hours,
145 cells were disrupted by sonication and clarified by filtration (GF/F Whatman). Analysis was
146 carried out by HPLC (Agilent Technologies 1200) immediately after clarification. For C3-L and
147 C4-L, 6.54 ml of culture were filtered in triplicates every 2 hours onto glass-fiber filters
148 (Whatman GF/C) precombusted at 450°C for 12h. Samples were kept at -80°C until analyses.
149 Filters were extracted in acetone (3 ml) for 1 hour at 4°C in the dark, with frequent and
150 gentle stirring. After 5 min of centrifugation (JOUAN G 412) at 2000 rpm, supernatant was
151 analyzed with a spectrophotometer (Perkin Elmer UV/Vis Spectrophotometer Lambda2).
152 Chlorophyll a, b and total carotenoids concentrations were determined reading absorbance
153 at 470.0, 644.8 and 661.6 nm and resolving the system described by Lichtenthaler [19] using
154 pure acetone. The variability between triplicates was lower than 7%.

155 **2.7 Statistical analysis**

156 Standard deviation was calculated using physical duplicates of the bioreactors (C1-LT, C2-LT
157 and C3-L, C4-L). The two successive periods of 24 hours were superimposed. Finally, the
158 presented points over 24 hours are the average over the two cycles and the duplicate
159 reactors. The hypothesis of linear correlation was accepted considering a p-value > 0.05.

160 **3. Results**

161 **3.1. Light and temperature variations.** Fig. 1 presents the variations of light and
162 temperature in this experiment. It was noticeable that diel variations of temperature were
163 able to reach high amplitudes, ranging from 24 to 33°C. The maximum of temperature (33°C)
164 occurred at the end of the light period, whereas the minimum was reached at the end of the
165 dark period. Contrary to the light regime, temperature variation was not symmetrical as it
166 increased faster than it decreased.

	C-LT		C-L	
	C1-LT	C2-LT	C3-L	C4-L
Maximum light intensity ($\mu\text{mol.m}^{-2}.\text{s}^{-1}$)	278	289	297	273
Light pattern	Sinus square function 14L:10D			
Temperature (°C)	Periodic variations (24.4°C - 32.9°C)		Constant (27°C)	
Dilution rate (d-1)	0.69	0.70	0.42	0.45
Average cell concentration (cell/L)	2.01×10^8	2.24×10^8	2.20×10^8	2.51×10^8

167

168 Table 1 : Experimental conditions applied to the different continuous cultures.

169

170 **3.2. Cell number and diameter**

171 Cell division in C-LT as in C-L cultures occurred preferentially during the dark period with a
172 major event of cell division at the end of the dark period (Fig. 2A). This shows that
173 populations were partially synchronized by the light cycles. In C-LT, cell number increased
174 during the dark period by 32 ± 4.7 %. Cell diameter increased quickly during the light period
175 in C-LT, reflecting the important somatic growth induced by carbon photosynthetic fixation.
176 It decreased more slowly during the dark period, reflecting both carbon respiration and cell
177 division. Cell diameters increased only several hours after the onset of the light period, as

178 cell division was still active during this time. Average cell diameter was significantly higher
 179 for C-LT ($9.62 \pm 0.01 \mu\text{m}$) than for C-L ($8.54 \pm 0.01 \mu\text{m}$; Fig. 2B).

180

181 **3.3. C and N fixation**

182 The daily-averaged carbon fixation rate (ρ_C) in C-LT was $0.66 \pm 0.036 \mu\text{gC} \cdot \mu\text{gC}^{-1} \cdot \text{d}^{-1}$. ρ_C values
 183 were lower in C-L, $0.53 \pm 0.048 \mu\text{gC} \cdot \mu\text{gC}^{-1} \cdot \text{d}^{-1}$ in accordance with lower division rate. In the C-
 184 LT cultures, ρ_C was strongly correlated with the light intensity ($R^2 > 0.99$, p-value > 0.01 , n $>$
 185 20) with a maximum value observed just before noon, leading to a significant increase of cell
 186 C during the light period. The same trend was observed in C-L cultures ($R^2 > 0.95$, p-value $>$
 187 0.01, n > 20 ; Fig. 3 A; Fig. 3 C; Fig. 6). At the end of the dark period, the respiration was
 188 responsible for C loss averaging $14.5 \pm 2.9 \%$ and $12.9 \pm 0.48 \%$ of the carbon accumulated
 189 during the previous 14h light phase, respectively in the C-LT and C-L cultures. Nitrogen
 190 fixation rate ρ_N was between five and tenfold lower than carbon fixation rate in all
 191 experiments (Table 2). In the C-LT cultures, nitrogen fixation also presented a diel cycle,
 192 leading to a significant increase of cell nitrogen during the light period (Table 2), but in
 193 contrast to carbon, significant fixation rates were also observed during the dark period (Fig.
 194 3B). For the C-L cultures, nitrogen fixation rate followed approximately the same trend but
 195 with much lower rates (Fig. 3D).

	C1-LT	C2-LT	C3-L	C4-L
	C-LT		C-L	
Carbon fixation rate ($\mu\text{gC} \cdot \mu\text{gC}^{-1} \cdot \text{d}^{-1}$)	0.66 \pm 0.036		0.53 \pm 0.048	
Nitrogen fixation rate ($\mu\text{gN} \cdot \mu\text{gC}^{-1} \cdot \text{d}^{-1}$)	0.094 \pm 0.010		0.069 \pm 0.012	
Min cell carbon quota ($\mu\text{gC} \cdot \text{cell}^{-1}$)	8.89 \pm 0.62 $\times 10^{-5}$		9.34 \pm 0.48 $\times 10^{-5}$	
Max cell carbon quota ($\mu\text{gC} \cdot \text{cell}^{-1}$)	1.49 \pm 0.2 $\times 10^{-4}$		1.76 \pm 0.13 $\times 10^{-4}$	
Min cell nitrogen quota ($\mu\text{gN} \cdot \text{cell}^{-1}$)	1.49 \pm 0.14 $\times 10^{-5}$		1.4 \pm 0.08 $\times 10^{-5}$	

Max cell nitrogen quota ($\mu\text{gN}\cdot\text{cell}^{-1}$)	$2.11 \times 10^{-5} \pm 0.22 \times 10^{-5}$		$2.36 \pm 0.17 \times 10^{-5}$	
N dark period fixation (%) on 24h	19.0 ± 2.54		25.0 ± 1.17	
C dark period losses (%) on the previous 14h of light period	14.5 ± 2.9		12.9 ± 0.48	
24h C fixation ($\mu\text{gC}\cdot\mu\text{gC}^{-1}$)	0.66 ± 0.031		0.43 ± 0.0099	
14h light period C fixation ($\mu\text{gC}\cdot\mu\text{gC}^{-1}$)	0.76 ± 0.043		0.51 ± 0.025	
10h dark period C fixation ($\mu\text{gC}\cdot\mu\text{gC}^{-1}$)	-0.10 ± 0.028		-0.06 ± 0.018	
Max TAG quota ($\mu\text{g}\cdot\mu\text{gC}^{-1}$)	$1.8 \pm 0.013 \times 10^{-2}$	$8.7 \times 10^{-3} \pm 1.8 \times 10^{-3}$	NA	NA
Min TAG quota ($\mu\text{g}\cdot\mu\text{gC}^{-1}$)	$5.5 \pm 1.0 \times 10^{-3}$	$3.21 \pm 0.34 \times 10^{-3}$	NA	NA
Max carotenoids quota ($\mu\text{g}\cdot\mu\text{gC}^{-1}$)	$4.52 \pm 0.23 \times 10^{-3}$	NA	NA	NA
Min carotenoids quota ($\mu\text{g}\cdot\mu\text{gC}^{-1}$)	$2.96 \pm 0.048 \times 10^{-3}$	NA	NA	NA

196

197 Table 2 : evolution of the different rates cell quotas (\pm standard deviation).

198

199 **3.4. Chlorophylls and carotenoids.**

200 The pigments to carbon ratio (Fig. 4 A, B) increased during the dark period and decreased
 201 sharply at the beginning of the light period. During the dark period, the amount of pigments
 202 per cell did not change significantly until cell division induced significant reduction (data not
 203 shown). In all experiments, the Carotenoids: Chlorophyll ratio reached its maximum value a
 204 few hours after the light maximum (Fig. 4 C).

205 **3.5. Lipid response in C-LT cultures**

206 Total lipids represented about $32 \pm 4.8\%$ of the cell carbon. In C-LT, the main lipid class was
 207 polar lipids. They represented $85 \pm 3.3\%$, of total lipids, and were constitutive of cell
 208 membranes (phospholipids, glycolipids, galactolipids...). B-carotene and triglycerides
 209 contributed for $5 \pm 3\%$ and $3 \pm 1\%$ of total lipids, respectively. This distribution was
 210 conserved during the L/D cycle. The polar lipids: carbon ratio showed small diel variations (\pm

211 13 %) in response to the L/D regime, but the variations were much more marked for the
212 triglycerides ($\pm 36\%$; Fig. 5). Triglyceride concentrations increased throughout the light
213 period reaching a maximum at the beginning of the dark period, and then decreased during
214 the dark period (Table 2). Triglycerides by carbon unit were higher in C1-LT than in C2-LT.

215 **4. Discussion**

216 **4.1. Responses of nitrogen and carbon quotas to light and temperature**

217 In all experimental conditions, the specific carbon fixation rate ρ_C was tightly linked with the
218 photon flux density (PFD), and the maximum fixation rate coincided with the light peak (Fig
219 3A, 3C). The linear relationship between ρ_C and PFD suggests that the light level applied to
220 the cultures was neither saturating nor photo-inhibiting (Fig. 6). In contrast, nitrogen fixation
221 rate ρ_N was much less correlated with PFD, even if higher rates were observed during the
222 light period (Fig 3C, 3D). This reflects the fact that, in non-limited cultures, nitrogen fixation
223 is principally controlled by both the energetic status and the cell cycle [2]. In the current
224 experiments, the decrease in nitrogen fixation during the dark phase could be partly
225 explained by the very low level of carbon storage. Since the energy and carbon necessary for
226 dark fixation of nitrogen can also be provided by the respiration of carbohydrates (not
227 measured), it is questionable to attribute the decrease in nocturnal nitrogen fixation to the
228 low level of triglycerides reached during the night, even if this status can potentially
229 contribute to the depression of dark nitrogen fixation. Another not exclusive explanation is
230 that nitrogen fixation is repressed during mitosis just before cell division [2].

231 The C:N ratio in the CL-T cultures was maximum at the end of the light period, i.e. when
232 temperature and level of stored lipids were maximal, and nitrogen uptake begins to

233 decrease. The C:N ratio was not influenced by temperature. There was no difference in the
234 C:N ratio between C-LT and C-L across the L/D cycle.

235 **4.2. Why the growth rate difference between C-LT and C-L?**

236 Despite the fact that the same light regime was applied to the cultures, the daily net carbon
237 fixation rate was significantly higher in C-LT than in the C-L culture, i.e. by 25% (Tab. 2). Such
238 a marked difference of carbon fixation rates between 2 sets of cultures where the daily
239 averaged temperature differed by only 1.8°C was clearly unexpected. Using the data of [9]
240 for *D. Salina* and the model of [20], it was shown that, all things being equal, a difference of
241 1.8°C can change the growth rate by about $\pm 10\%$, which is much less than the +25%
242 observed in this study. Our hypothesis to explain this discrepancy may be that the
243 temperature in C-LT cultures was not constant but cycling. Indeed, some authors have
244 shown that periodic light variations increased growth rate when compared with constant
245 conditions [21]. Temperature could act similarly. Towards a better understanding of the
246 underlying phenomena, we examine here if the differences of measured carbon fixation and
247 dark respiration between C-LT and C-L cultures can explain their difference in net carbon
248 fixation.

249 Firstly, it is worth noting that the difference in ρ_c between C-LT and C-L cultures increased
250 when PFD exceeded $100 \mu\text{mol quanta}\cdot\text{m}^{-2}\cdot\text{sec}^{-1}$. The difference was maximum at $300 \mu\text{mol}$
251 $\text{quanta}\cdot\text{m}^{-2}\cdot\text{sec}^{-1}$ (Fig. 6). This also corresponded to higher temperatures in C-LT than in C-L.
252 During this part of the light period, the carbon fixation rate was more stimulated in the C-LT
253 cultures by high temperatures, leading to a 50% higher total amount of carbon fixed than in
254 C-L (Table2). This suggests that the temperature increase in C-LT during the light period had

255 a clear positive synergetic effect on carbon fixation, compared to C-L at this temperature
256 range.

257 Secondly, the potential difference in respiration for different temperature regimes during
258 the dark period may explain the difference between C-LT and C-L. Under L/D cycle and
259 constant temperature, the dark respiration rate is dependent on both the light phase
260 duration and light intensity, and is also correlated to the incubation temperature by an
261 Arrhenius law [22]. Under dynamic temperature variations, respiration during the dark
262 period was still correlated to the temperature through the same relationship, with a high
263 level of confidence ($R^2 = 0.70$, $p\text{-value} > 0.05$, $n > 20$, C-LT; Fig. 7). This is not surprising as
264 respiration is under the control of enzymes that are tightly controlled by temperature [23].
265 In C-L cultures, such a relationship could not be revealed, as the temperature was
266 maintained constant at 27°C. Mean respiration rates were lower in C-L than in C-LT cultures,
267 confirming the fact that under L/D cycles, respiration is related to the temperature
268 experienced during the light period [22].

269 In conclusion, the higher temperature during the light period in C-LT leads to a higher
270 carbon fixation rate and a higher respiration rate during the dark period than in C-L. The
271 resulting balance of these opposite terms was a higher net C fixation in C-LT.

272 ***4.3. Lipid storage: a consequence of C-N imbalance uptake in C-LT***

273 In non-limiting conditions, the major lipid class is polar lipids (Fig. 5). In agreement with [3],
274 polar lipids per carbon unit did not significantly change during the L/D cycle, whereas polar
275 lipids per cell showed a marked minimum observed during the major cell division event (dark
276 period). This preponderantly membrane lipid class is related to cell volume that varied
277 during the L/D cycle ($R^2 = 0.83$, $p\text{-value} < 0.01$, $n = 14$). In C-LT, the total lipid content was 32

278 $\pm 4.8 \mu\text{g}\cdot\mu\text{gC}^{-1}$ on average (representing 17 % in dry weight, calibration curves not shown), in
279 accordance with the data of [24]. The contribution of energetic lipids, mainly triglycerides,
280 represented only 5% of the total lipid, confirming that under replete nitrogen conditions,
281 triglycerides are not the main form of carbon storage in this strain of *Dunaliella*. The amount
282 of triglycerides per carbon unit reached a maximum at the end of the light period. This
283 reflects the imbalance between nitrogen and carbon fixations observed during the light
284 period (Tab. 2) where the excess of fixed carbon could be reallocated in N-free molecules
285 like triglycerides. This mechanism similarly drives the lipid accumulation in nitrogen
286 starvation [25]. In this scenario, cells adapt to the diel cycle by using the energy stored
287 during the light period to proceed to division during the dark phase.

288 **4.4. Pigment evolution across a light dark cycle**

289 To our knowledge, no data on carotenoids evolution across a L/D cycle has been published
290 for *D. salina*. In C-LT, the measured concentrations of beta-carotene per carbon unit reached
291 an average value of $0.004 \mu\text{g}\cdot\mu\text{gC}^{-1}$ (2% of the dry weight), that is 10-fold lower than the
292 measurements of [9] measured at constant light. This unexpected low level cannot be solely
293 explained by the replete nitrogen conditions in our experiment, but is also probably a
294 characteristic of the chosen strain. There was an increase of beta-carotene content per
295 carbon unit during the dark period due to a decrease in carbon by respiration. This
296 corresponded to a specific beta-carotene fixation rate high and constant ($0.7 \mu\text{g}_{\text{Beta-Carotene}}\cdot\mu\text{g}_{\text{Beta-Carotene}}\cdot\text{d}^{-1}$). At the end of the dark period, during cell division, this increase
297 ceased and the pigment content per carbon unit decreased corresponding to a sharp
298 decrease in the specific beta-carotene fixation rate until the value of $0.5 \mu\text{g}_{\text{Beta-Carotene}}\cdot\mu\text{g}_{\text{Beta-Carotene}}\cdot\text{d}^{-1}$. The same behavior was observed for all the pigments except zeaxanthin. Beta-

301 carotene did not play any role in respiration. Under L/D cycle and nitrogen replete
302 conditions, beta-carotene does not function as carbon storage molecules, in contrast to
303 what happens during nitrogen starvation [26]. Moreover, in synchronized cultures, beta-
304 carotene, as the other pigments, was continuously produced by cells except during the cell
305 division event when nitrogen acquisition stopped [2]. The carotenoids:chlorophylls a
306 (car:chl_a) ratio has been suggested as a possible indicator of stress level [24, 5]. In previous
307 nitrogen deprivation experiments, with constant light and temperature, a car:chl_a ratio of
308 13.2 was reached, whereas for nitrogen replete cultures, a ratio of 0.52 was measured (data
309 not shown). In C-LT, the car:chl_a ratio evolved between $0.58 \pm 1.23 \times 10^{-2}$ g:g at the beginning
310 of the light period to $0.62 \pm 9.13 \times 10^{-3}$ g:g, whereas, the evolution was between $0.34 \pm 9 \times 10^{-3}$
311 g:g and $0.38 \pm 4 \times 10^{-3}$ g:g g/g in C-L (Fig. 4). These low ratios confirmed the absence of photo-
312 limitation in this experiment. The increase of this ratio was concomitant with light and
313 reached its maximum a few hours after the light maximum. The temperature evolution did
314 not seem to have impacted this ratio but the sampling frequency was probably too low to
315 observe significant differences.

316 **5. Conclusion**

317 This study highlights the growth dynamics of *D. salina* under diel fluctuations of light and
318 temperature, and provides some insights towards understanding the growth dynamics under
319 realistic outdoor conditions. In particular, the importance of temperature variations on cell
320 metabolism is highlighted, suggesting that this parameter should be more often taken into
321 account in addition to light in experimental studies. Additional realistic experiments should
322 support modeling attempts, since, to date, there is no reliable model able to predict algae

323 production in outdoor cultivation systems subjected to concomitant and large variations of
324 light and temperature.

325 **6. Acknowledgements:**

326 H. Bonnefond acknowledges the support of an ADEME grant. The experiments were carried
327 out in the framework of the FUI Salinalgue project. He equally gratefully acknowledges B.
328 Rémond for her kind help during sampling and Q. Béchet for his intellectual honesty.

329 **7. References cited**

- 330 [1] J. Spudich, R. Sager, Regulation of the *Chlamydomonas* cell cycle by light and dark., *J. Cell Biol.* 85
331 (1980). <http://jcb.rupress.org/content/85/1/136.abstract> (accessed December 29, 2014).
- 332 [2] C. Mocquet, A. Sciandra, A. Talec, O. Bernard, Cell cycle implication on nitrogen acquisition and
333 synchronization in *Thalassiosira weissflogii* (Bacillariophyceae), *J. Phycol.* 49 (2013) 371–380.
334 doi:10.1111/jpy.12045.
- 335 [3] T. Lacour, A. Sciandra, A. Talec, P. Mayzaud, O. Bernard, Diel Variations of Carbohydrates and Neutral
336 Lipids in Nitrogen-Sufficient and Nitrogen-Starved Cyclostat Cultures of *Isochrysis* Sp.1, *J. Phycol.* (2012)
337 no–no. doi:10.1111/j.1529-8817.2012.01177.x.
- 338 [4] A. Sukenik, Y. Carmeli, Lipids synthesis and fatty acid composition in *Nannochloropsis* sp.
339 (EUSTIGMATOPHYCEAE) grown in a light dark cycle, *J. Phycol.* 26 (1990) 463–469.
- 340 [5] H. Chen, J.-G. Jiang, G.-H. Wu, Effects of salinity changes on the growth of *Dunaliella salina* and its
341 isozyme activities of glycerol-3-phosphate dehydrogenase., *J. Agric. Food Chem.* 57 (2009) 6178–82.
342 doi:10.1021/jf900447r.
- 343 [6] a Ben-Amotz, M. Avron, On the Factors Which Determine Massive beta-Carotene Accumulation in the
344 Halotolerant Alga *Dunaliella bardawil*., *Plant Physiol.* 72 (1983) 593–7.
345 <http://www.pubmedcentral.nih.gov/articlerender.fcgi?artid=1066285&tool=pmcentrez&rendertype=abstract>.
346
- 347 [7] P. Spolaore, C. Joannis-Cassan, E. Duran, A. Isambert, Commercial applications of microalgae., *J. Biosci.*
348 *Bioeng.* 101 (2006) 87–96. doi:10.1263/jbb.101.87.
- 349 [8] Q. Béchet, A. Shilton, J.B.K. Park, R.J. Craggs, B. Guieysse, Universal Temperature Model for Shallow
350 Algal Ponds Provides Improved Accuracy, *Environ. Sci. Technol.* 45 (2011) 3702–9.
351 doi:10.1021/es1040706.
- 352 [9] F. García, Y. Freile-Pelegrín, D. Robledo, Physiological characterization of *Dunaliella* sp. (Chlorophyta,
353 Volvocales) from Yucatan, Mexico., *Bioresour. Technol.* 98 (2007) 1359–65.
354 doi:10.1016/j.biortech.2006.05.051.

- 355 [10] P.P. Lamers, C.C.W. van de Laak, P.S. Kaasenbrood, J. Lorier, M. Janssen, R.C.H. De Vos, et al.,
356 Carotenoid and fatty acid metabolism in light-stressed *Dunaliella salina*., *Biotechnol. Bioeng.* 106 (2010)
357 638–48. doi:10.1002/bit.22725.
- 358 [11] R. Guillard, Culture of phytoplankton for feeding marine invertebrates, *Cult. Mar. Invertebr. Anim.*
359 *Plenum.* (1975) 1975.
360 <http://scholar.google.com/scholar?hl=en&btnG=Search&q=intitle:Culture+of+phytoplankton+for+feeding+marine+invertebrates#0> (accessed October 3, 2012).
361
- 362 [12] E. Le Floch, G. Malara, A. Sciandra, An automatic device for in vivo absorption spectra acquisition and
363 chlorophyll estimation in phytoplankton cultures, (2003) 435–444.
- 364 [13] O. Bernard, F. Mairet, Modelling of Microalgae Culture Systems with Applications to Control and
365 Optimization, *Adv. Biochem. Eng.* (2015).
- 366 [14] H. Takache, G. Christophe, J.-F. Cornet, J. Pruvost, Experimental and theoretical assessment of
367 maximum productivities for the microalgae *Chlamydomonas reinhardtii* in two different geometries of
368 photobioreactors., *Biotechnol. Prog.* 26 (2010) 431–40. doi:10.1002/btpr.356.
- 369 [15] A. Savitzky, M. Golay, Smoothing and differentiation of data by simplified least squares procedures.,
370 *Anal. Chem.* 36 (1964) 1627–1639. <http://pubs.acs.org/doi/abs/10.1021/ac60214a047> (accessed
371 October 6, 2014).
- 372 [16] O. Bernard, G. Malara, A. Sciandra, The effects of a controlled fluctuating nutrient environment on
373 continuous cultures of phytoplankton monitored by computers, *J. Exp. Mar. Bio. Ecol.* 197 (1996) 263–
374 278. doi:10.1016/0022-0981(95)00161-1.
- 375 [17] E. Bligh, W. Dyer, A rapid method of total lipid extraction and purification, *Can. J. Biochem. Physiol.* 37
376 (1959) 911–917. <http://www.nrcresearchpress.com/doi/abs/10.1139/o59-099> (accessed March 22,
377 2012).
- 378 [18] R. Ackman, Flame ionization detection applied to thin-layer chromatography on coated quartz rods,
379 *Methods Enzymol.* (1981). <http://www.sciencedirect.com/science/article/pii/S0076687981720135>
380 (accessed November 6, 2012).
- 381 [19] H. Lichtenthaler, Chlorophylls and carotenoids: Pigments of photosynthetic biomembranes, *Methods*
382 *Enzymol.* 148 (1987) 350–382. <http://www.sciencedirect.com/science/article/pii/0076687987480361>
383 (accessed March 13, 2012).
- 384 [20] O. Bernard, B. Rémond, Validation of a simple model accounting for light and temperature effect on
385 microalgal growth., *Bioresour. Technol.* 123 (2012) 520–7. doi:10.1016/j.biortech.2012.07.022.
- 386 [21] M. V. Nielsen, Irradiance and daylength effects on growth and chemical composition of *Gyrodinium*
387 *aureolum* Hulburt in culture, *J. Plankton Res.* 14 (1992) 811–820. doi:10.1093/plankt/14.6.811.
- 388 [22] J. Grobbelaar, C. Soeder, Respiration losses in planktonic green algae cultivated in raceway ponds, *J.*
389 *Plankton Res.* 7 (1985) 497–506. <http://plankt.oxfordjournals.org/content/7/4/497.short> (accessed
390 October 7, 2014).
- 391 [23] N. Devos, M. Ingouff, R. Loppes, R.F. Matagne, Rubisco adaptation to low temperatures: a comparative
392 study in psychrophilic and mesophilic unicellular algae, *J. Phycol.* 34 (1998) 655–660.
393 doi:10.1046/j.1529-8817.1998.340655.x.
- 394 [24] M.J. Griffiths, S.T.L. Harrison, Lipid productivity as a key characteristic for choosing algal species for
395 biodiesel production, *J. Appl. Phycol.* 21 (2009) 493–507. doi:10.1007/s10811-008-9392-7.

- 396 [25] M. Vítová, K. Bišová, S. Kawano, V. Zachleder, Accumulation of energy reserves in algae: From cell
397 cycles to biotechnological applications, *Biotechnol. Adv.* (2015). doi:10.1016/j.biotechadv.2015.04.012.
- 398 [26] P.P. Lamers, M. Janssen, R.C.H. De Vos, R.J. Bino, R.H. Wijffels, Exploring and exploiting carotenoid
399 accumulation in *Dunaliella salina* for cell-factory applications., *Trends Biotechnol.* 26 (2008) 631–8.
400 doi:10.1016/j.tibtech.2008.07.002.
- 401 [27] E. Young, J. Beardall, Photosynthetic function in *Dunaliella tertiolecta* (Chlorophyta) during a nitrogen
402 starvation and recovery cycle, *J. Phycol.* 905 (2003) 897–905.
403 <http://onlinelibrary.wiley.com/doi/10.1046/j.1529-8817.2003.03042.x/full> (accessed January 30, 2013).

404

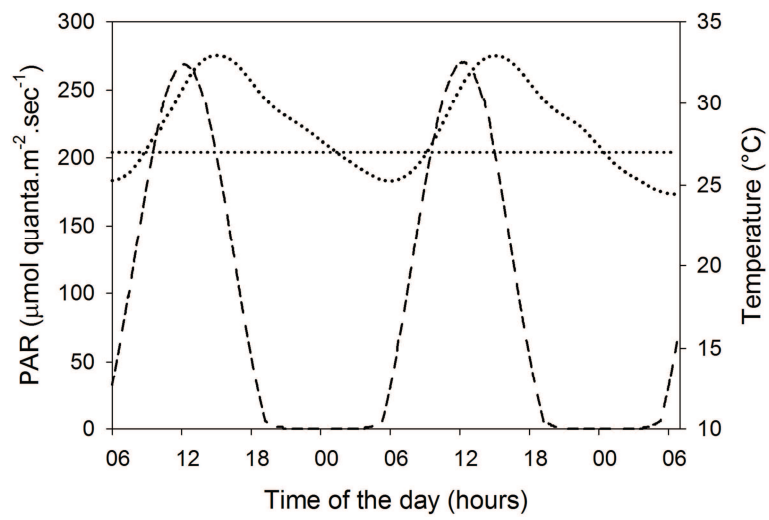


Figure 1. PAR (dashed line) applied to cultures C-LT and C-L. Temperature was maintained constant at 27°C in C-L cultures (horizontal dotted line), whereas it varied in C-LT cultures (dotted curve).

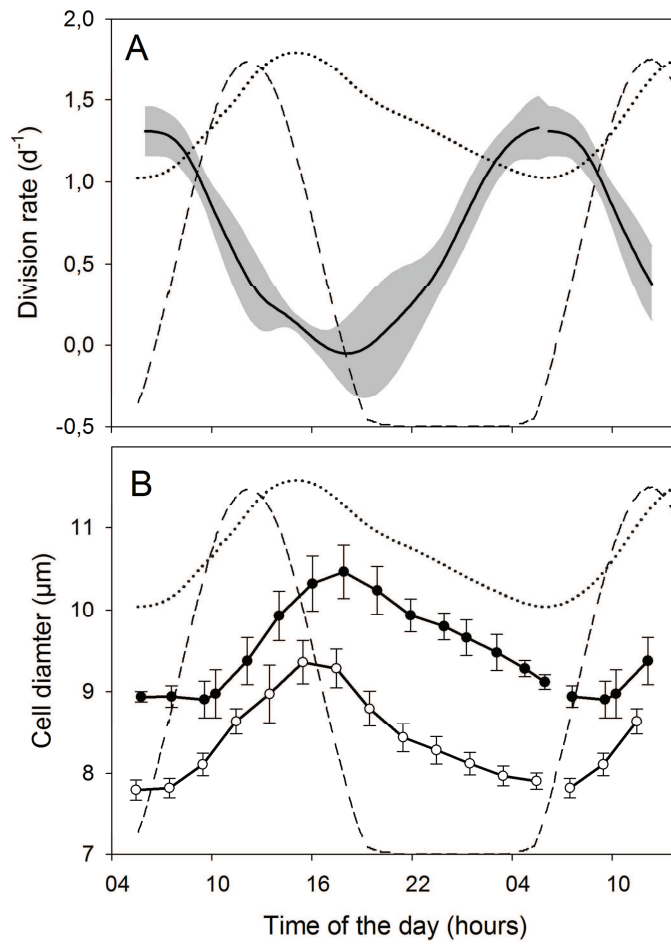


Figure 2. **A:** mean cell division rate (continuous black line) +/- one SD (grey area) in C-LT cultures. **B:** mean cell diameter in C-LT (closed symbol) and C-L (open symbol) cultures. Temperature variation (dotted line), light variation (dashed line).

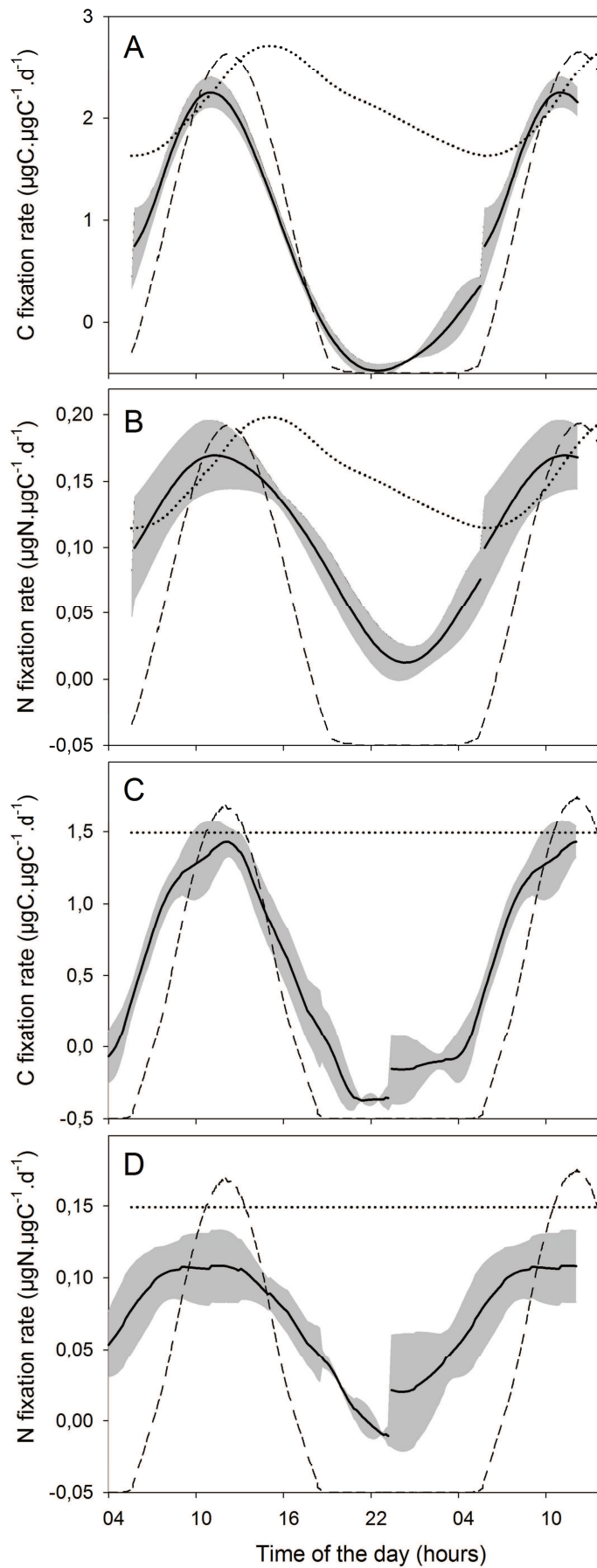


Figure 3. Averaged values of carbon fixation rate in C-LT (A) and C-L (C) cultures, and of nitrogen fixation rates in C-LT (B) and C-L (D) cultures. Temperature variation (dotted line), light variation (dashed line).

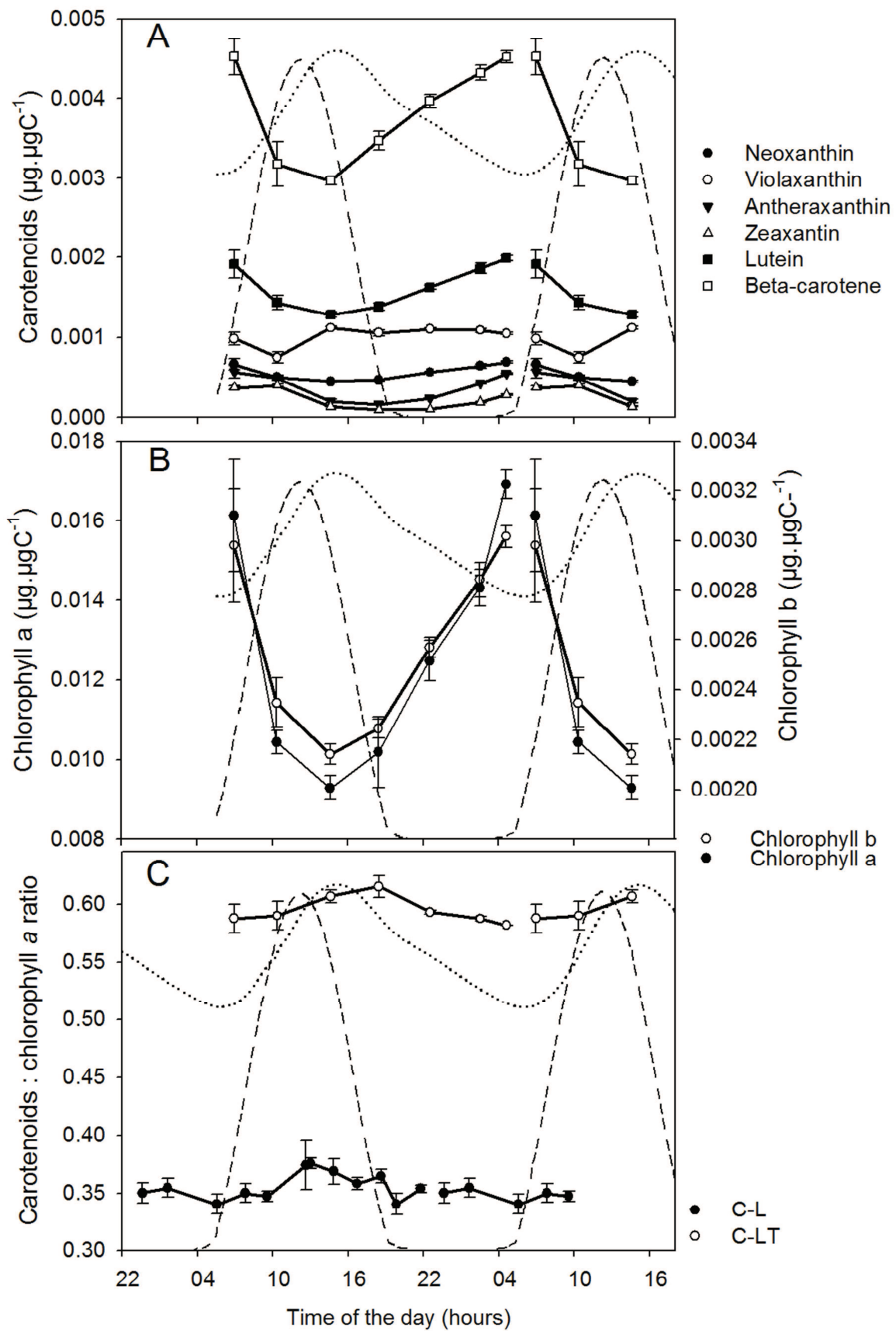


Figure 4. **A:** quota of xanthophylls and beta-carotene in C-LT cultures. **B:** quotas of chlorophylls *a* and *b* in C-LT cultures. **C:** carotenoids:chlorophyll *a* ratio in C-L and C-LT cultures. Temperature variation (dotted line), light variation (dashed line).

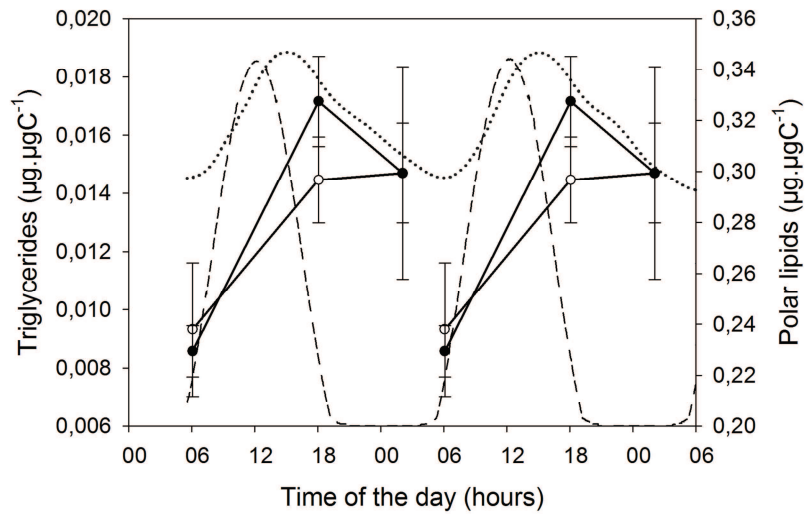


Figure 5. Quotas of polar lipids (open symbol) and triglycerides (closed symbol) in C-LT cultures. Temperature variation (dotted line), light variation (dashed line).

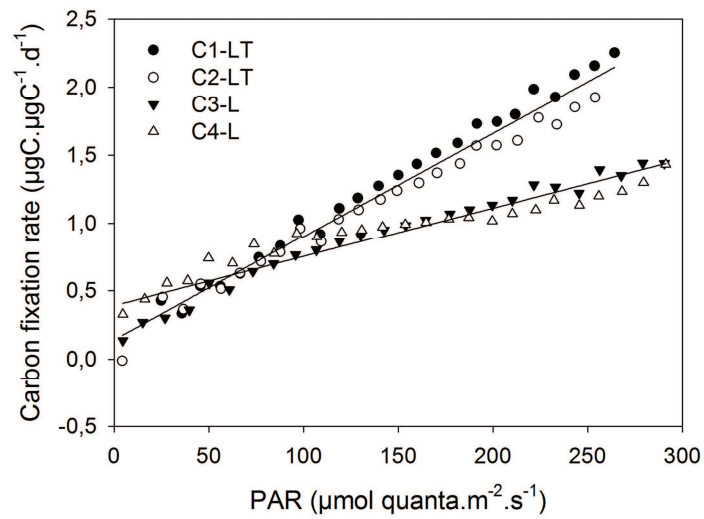


Figure 6. Correlation between the specific carbon fixation rate and PAR in C-LT and C-L cultures.

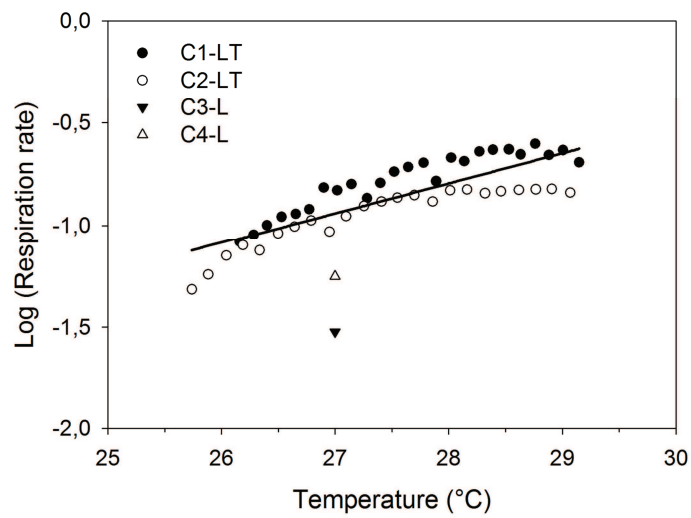


Figure 7. Arrhenius plots of respiration rate measured during the dark period only, in C-LT and C-L cultures.